

MANU-CHAO: A laboratory Ground-Layer Adaptive Optics Experiment

Sebastian E. Egner^a, Wolfgang Gaessler^a, Roberto Ragazzoni^b, Brice LeRoux^c,
T.M. Herbst^a, J. Farinato^b, E. Diolaiti^d, C. Arcidiacono^b

^aMax-Planck-Institute for Astronomy, Koenigstuhl 17, 69117 Heidelberg, Germany;

^bINAF - Osservatorio Astrofisico di Padova, Vicolo dell'Osservatorio 5, 35122 Padova, Italy;

^cINAF - Osservatorio Astrofisico di Arcetri, L.go E.Fermi 5, 50125 Firenze, Italy;

^dINAF - Osservatorio Astronomico di Bologna, via Ranzani 1, 40127 Bologna, Italy;

ABSTRACT

We present a laboratory setup of a Ground-Layer Adaptive Optics system. This system is a scaled-down version of the MCAO system of MAD (a MCAO system for the VLT) / LINC-NIRVANA (a Fizeau Imager for the LBT) and measures the wavefront aberrations with 4 pyramids in a layer-oriented fashion with optical co-addition. The laboratory setup contains besides the wavefront-sensing unit a telescope-simulator, a dynamic turbulence generator and a Deformable Mirror for the wavefront correction. We describe the overall system and its single components, open- and closed-loop measurements of the characteristics of a system working in GLAO mode and first results when using a Kalman filter for the control of the wavefront reconstruction process.

Keywords: Adaptive Optics, GLAO, Kalman filter, pyramid wavefront-sensor

1. INTRODUCTION

Turbulence in Earth's atmosphere significantly reduces the achievable image quality of large ground-based telescopes. In order to correct for the optical effects of this turbulence, the technique of Adaptive Optics (AO) was proposed already in the 1950s.¹ However, not before the early 1990s the technological challenges could be solved to use this method for astronomical observations. After a rapid development, today at almost every large ground-based telescope an AO system is in operation.

Classical AO system use one natural Guide-Star (GS) to measure the deformations of the incoming wavefront with a wavefront-sensor and correct them with the help of a Deformable Mirror (DM). However, the achievable correction is useful only in a small area around the Guide-Star, this so-called isoplanatic angle ϑ_0 is typically around 20" in K-Band. For objects outside this region, the wavefront aberrations are different from the ones measured (and thus corrected) with the Guide-Star, reducing the efficiency of the correction for these objects. Since the number of sufficiently bright Guide-Stars (typically brighter than 14mag in V) is relatively small, only a tiny fraction (around 1%) of the complete sky can be observed with classical AO system. To increase the size of the corrected area and thus the sky-coverage, the concept of Multi-Conjugate Adaptive Optics (MCAO) was proposed.^{2,3} For this method, several Guide-Stars are used to measure the turbulence in the complete 3d volume above the telescope. Several DMs are then placed optically at the altitudes of the most turbulent layers, and thus compensating the turbulence in single layers and no longer in a single direction. The result is that the maximum achievable performance on-axis is not as good as with Classical AO because of uncorrected turbulence in between the single corrected layers, but that the correction is much more uniform over the significantly increased field-of-view.

When considering the vertical profile of the optical turbulence, it turns out that most of the turbulence is in the first few hundred meters above the ground (see e.g. SCIDAR measurements at different astronomical sites: SPM,⁴ Mt. Graham,⁵ Pic du Midi,⁶ Mauna Kea⁷). This fact offers the prospect that a good correction can already be achieved when correcting only the effects of the turbulence in the Ground-Layer. For this reason, Rigaut⁸ proposed a "MCAO-light" system, i.e. to determine and correct only the ground-layer turbulence, thus

Send correspondence to S.E. Egner, E-mail: egner@mpia.de, phone: +49 (0) 6221 528 221

called Ground-Layer Adaptive Optics (GLAO). To separate the wavefront aberrations introduced by the ground-layer from the other high-altitude turbulent layers, there are two possibilities. One is to use artificial GS, created with a laser beacon at an altitude of only a few kilometers above the telescope, and thus sampling only the turbulence below the altitude of this Laser Guide-Star (LGS). This approach is currently being pursued by a number of observatories (e.g. for GMT,⁹ ESO,¹⁰ WHT,¹¹ SOAR¹²).

The other possibility is to use more than one GS (natural or Sodium-LGS) and then – similar to a full-fledged MCAO system – to retrieve from the correlation of the wavefront aberrations in the different directions, the wavefront aberrations introduced by the single layers. This method works in an elegant way when using a pupil plane wavefront sensor (like e.g. a pyramid) and the layer-oriented approach,^{13,14} where this separation into the different layers is done optically. In the case of a pyramid wavefront sensor, the wavefront camera is focused to the desired conjugation altitude and the pupil images of the single pyramids are overlapped on the detector according to their footprint at this conjugation altitude (see e.g. fig. 4).

Simulations for GLAO systems predict only a moderate Strehl-ratio, but a significantly reduced FWHM of the PSF over a rather wide field-of-view^{15,16} (depending on the number, position and altitude of the NGSs or LGSs). Such a GLAO system would be well suited for scientific applications where a diffraction-limited image is not required, but a significant gain is already achieved for an effective reduction of the seeing by a factor of around 2, like e.g. spectroscopy.

Open-loop measurements with a Shack-Hartmann wavefront sensor and using 4 stars have already demonstrated the principle.¹⁷ However, up to now, no GLAO or MCAO system using several natural guide-stars is running in closed loop. For this reason, and to measure the characteristics of such a GLAO system in a systematic way, we designed and set up a laboratory experiment, including all the relevant components (dynamic atmosphere simulator, Deformable Mirror, wavefront sensor unit (“MANU-CHAO”) and control software). With this system, we examined the effects of the non-conjugated layers on the measured wavefront, the sensitivity of matching the conjugation height of the DM / WFS combination to the atmospheric turbulence vertical structure and the performance increase when using advanced control algorithms.

2. THE LAB-SETUP

As mentioned above, the lab-setup contains all the components for a closed-loop GLAO system. The single components of our GLAO system will be described in detail in this section.

2.1. Optical Layout

The basic layout of MANU-CHAO consists of a light-source to simulate the guide-stars and the science object, a dynamic turbulence generator to emulate the optical turbulence in the atmosphere and some collimating optics to image the pupil on the deformable mirror. The reflected light from the DM is focused with another set of lenses to a telecentric F/32 beam, which is fed into the wavefront sensing unit, except for the light of the science object, which is reflected by a pick-off mirror to the science camera. A picture showing the complete setup is shown in figure 1.

2.2. Turbulence Generator

The used Turbulence Generator “Multiple Atmospheric Phasescreens and Stars” (MAPS) is described in great detail by Hippler et al.,¹⁸ thus only the basic characteristics are given here. MAPS has a symmetric design with two identical collimators manufactured by JANOS, with the first lens group collimating the light from several fibers at the front focal plane and creating a pupil image with a diameter of 13mm. The second collimator then focuses the light again onto the back focal plane. This back focal plane has the same characteristics (diameter, curvature, plate-scale) as the front focal plane. Without the phasescreens placed between the two collimators, the image quality is diffraction-limited over the complete field-of-view (70mm, corresponding to 2' at a 8m F/15 telescope) and over the wavelength range of 0.5 to 2.2 micron.

To emulate the atmospheric turbulence, we use rotating, etched glass plates manufactured by SILIOS with a diameter of 10cm. The desired wavefront aberrations were first simulated and then transferred to the glass-plates via a multi-layer etching technique. Up to three phasescreens can be inserted in MAPS, producing a seeing of

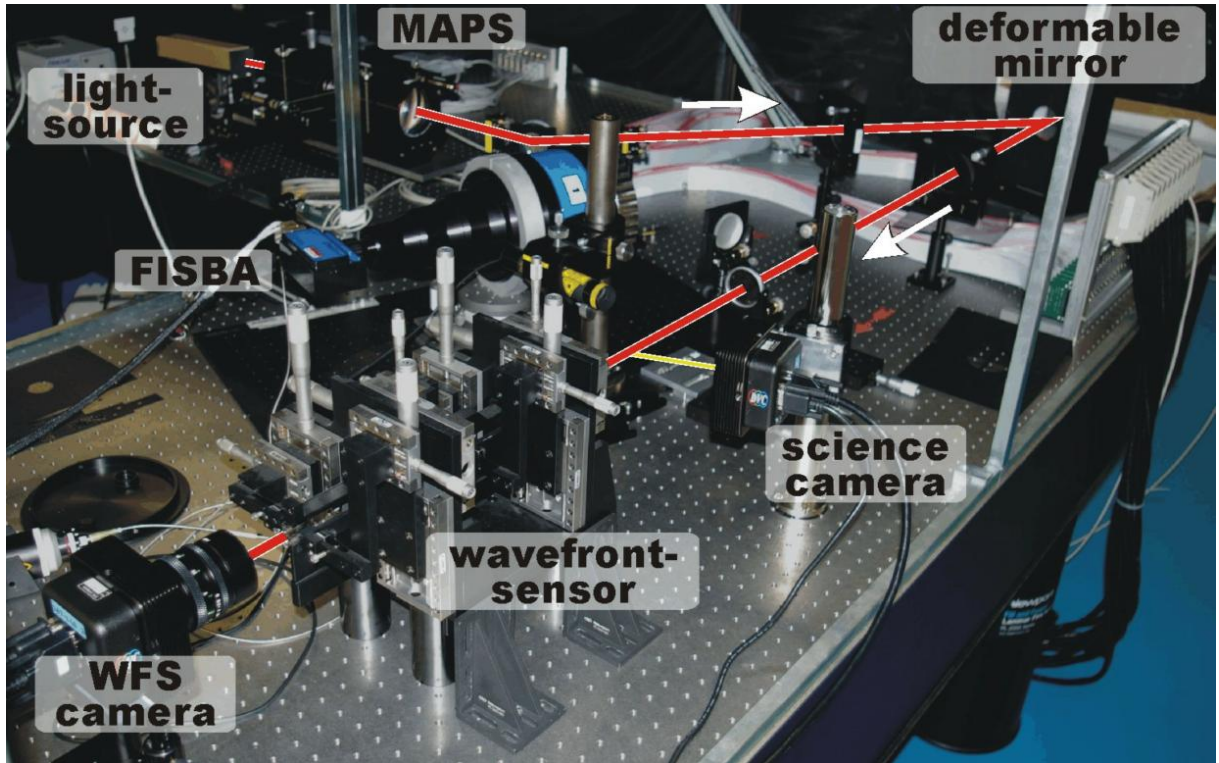


Figure 1. Picture showing the complete lab setup with light-source, turbulence generator (MAPS), collimating optics, Deformable Mirror, re-focusing optics, science camera and wavefront sensor unit (MANU-CHAO). The FISBA interferometer is used for calibration and monitoring purposes of the DM only.

between 0.3 and 1.5 arcsec in the visible. The altitude of the phasescreens can be adjusted continuously from 100m to 15km above the telescope, the temporal evolution of the turbulence is adjusted with the rotation speed of their motors.

As a light-source we used fibers with various diameters attached to a plate mounted at the front focal plane of MAPS. The fibers have diameters of 5 to 500 microns, corresponding to an angular size of diffraction limit to 0.85" for a F/15 8m telescope. The fibers with the larger diameter were used to emulate the effect of modulating the beam on the tip of the pyramid and to examine its effect on the performance. The fibers can be mounted to various positions in the field-of-view. For most of the measurements, the fibers for the GS were placed at the corners of a rectangular with 40"×35" and for the science object in the center of the rectangular. As the light-source for the GS, we used a white-light source attached to the fibers, for the science object we used a laser with a wavelength of 835nm.

2.3. Collimating Optics

To image the pupil onto the DM and to focus the reflected light as required for the wavefront sensing unit, we designed a collimating / refocusing optics. The requirements were to create a pupil image on the DM with a diameter of 65mm, to use commercially available lenses and to produce a diffraction-limited telecentric F/32 beam as a feed for the wavefront sensor unit. To keep the length short, and achieve diffraction-limited performance, each optics uses 3 lenses. A CAD drawing of the complete optical design including MAPS and the collimating / refocusing optics can be seen in figure 2.

2.4. Deformable Mirror

As the Deformable Mirror we use a continuous facesheet DM by Xinetics, which will later be used for LINC-NIRVANA,¹⁹ with a diameter of 150mm and 349 piezo-stack actuators. The characteristics like linearity, hystere-

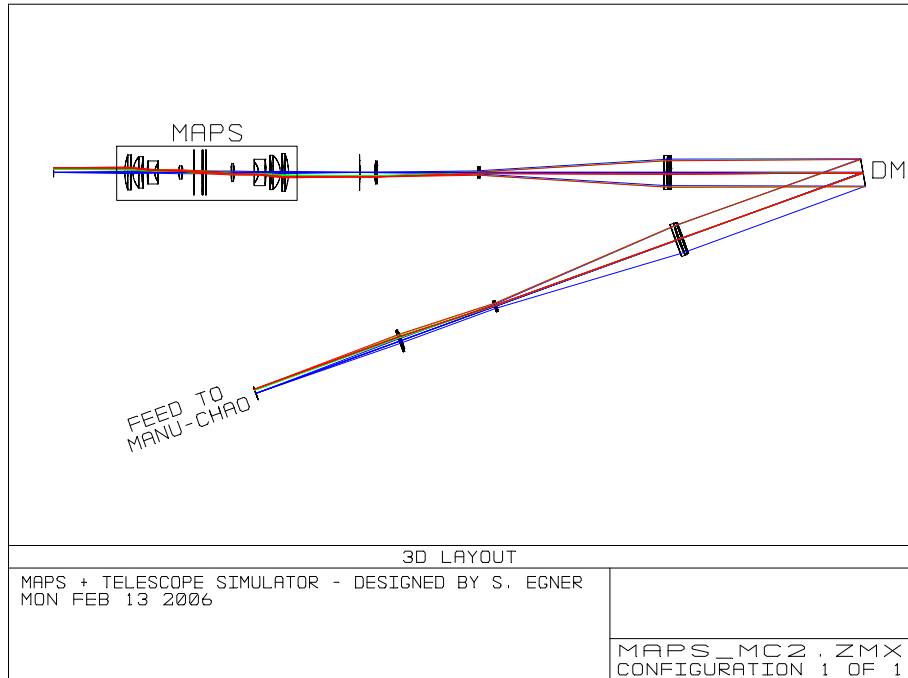


Figure 2. Optical design of the telescope simulator, including the turbulence simulator (MAPS), the collimator to image the pupil onto the DM and the telescope simulator to create the telecentric F/32 beam which is needed for the wavefront sensor unit (MANU-CHAO).

sis, gain and influence functions of all the actuators have been measured extensively²⁰⁻²² to guarantee optimal control. Together with the determination of the required voltages to get an optical flat mirror surface, the DM can routinely be controlled at room temperature to an accuracy of around $\lambda/20$ in the range of 75% of full stroke.

From the measured influence function of each actuator, we calculated the voltages which have to be applied to each actuator for a good representation of Zernike modes. But due to the lack of easy availability of large optical lenses for the lab setup, we only used an area with 65mm diameter on the DM and thus only around 100 actuators. The voltages for the unused actuators are calculated from the voltages of the used actuators by taking the mean voltage of the adjacent actuators. Furthermore, the excursions of the unused actuators are reduced by a factor of 2.0 for each ring of actuators from the inside to the outside. The voltages projected on the DM and a comparison to the theoretical Zernike modes are shown in figure 3.

For monitoring and security purposes, the DM is continuously watched with a commercial Twyman-Green Interferometer by FISBA Optics during closed-loop operation of the system. One measurement of the DM surface with the FISBA would take around 15 seconds and can thus not be done in real-time. However, we found it extremely useful to watch the fringes (which are displayed in real-time) during the operation of the AO system. In this way problems with single actuators or with the reconstruction process can be easily identified and examined. Furthermore, the FISBA is used for the calibration of the DM, like for example to determine the voltages required to get an optically flat mirror surface.

2.5. Wavefront-Sensor

As mentioned in the introduction, the wavefront sensor unit of MANU-CHAO is a layer-oriented system using four natural guide stars. MANU-CHAO uses four pyramids, a pupil re-imaging optics and one single wavefront camera to measure the wavefront aberrations.

To achieve a reasonable linear range of the pyramid, the size of the Airy disk has to be comparable to the size of the tip of the pyramid. This can be accomplished by increasing the F-ratio of the beam from in our case

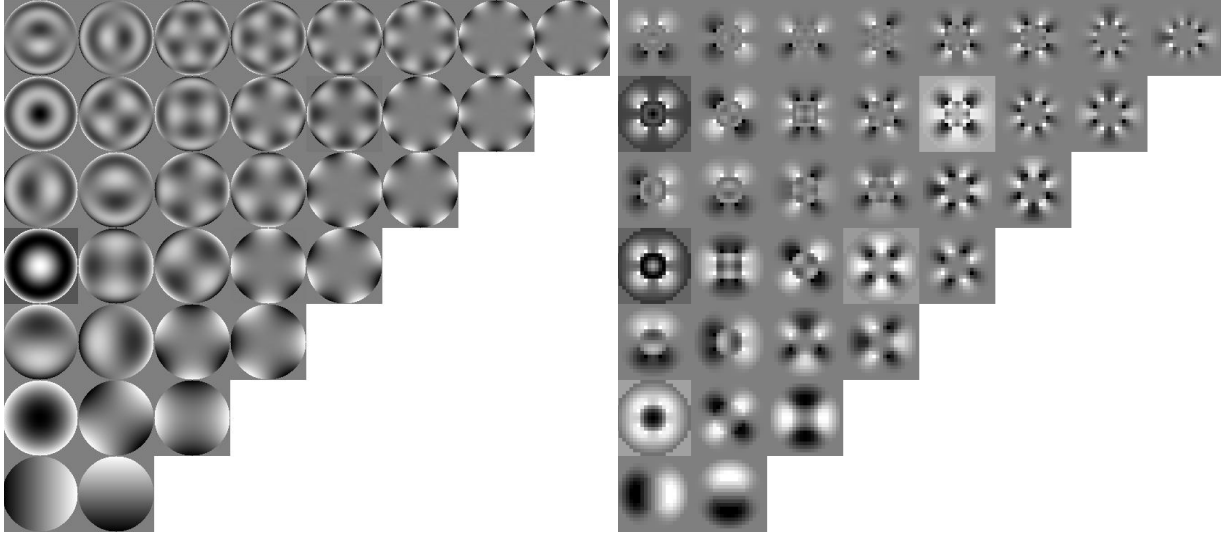


Figure 3. The theoretical Zernike modes (left) as compared to the actual projected modes on the DM (right). Only the inner 65mm (of the complete 150mm diameter) are used in MANU-CHAO. The unused actuators are set to the mean voltage of the adjacent actuators and multiplied with an attenuation factor of 0.5 for each ring from the inside to the outside.

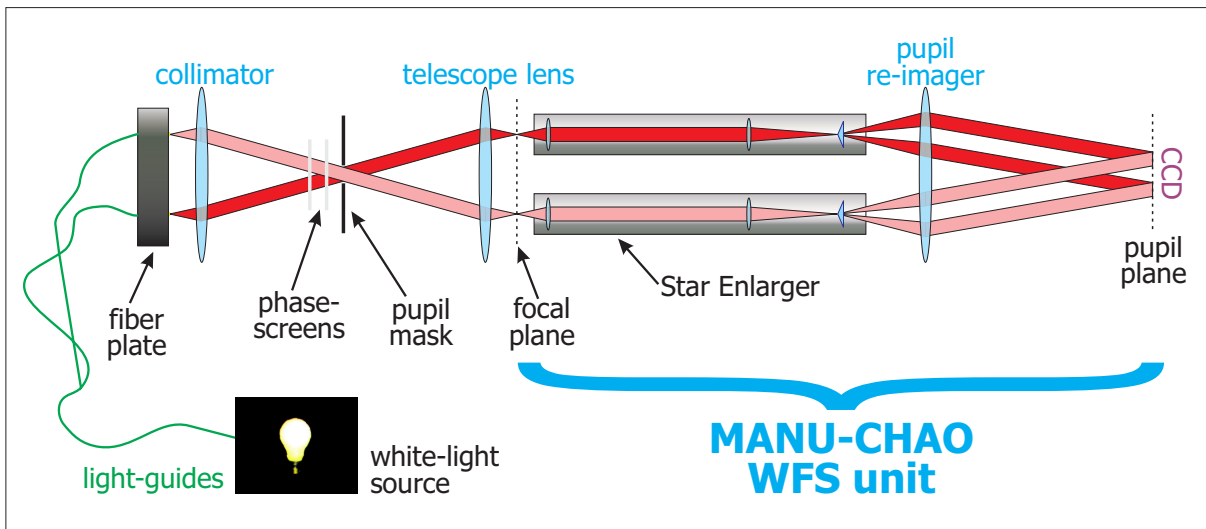


Figure 4. A very simplified sketch of the optical setup of MANU-CHAO (without the Deformable Mirror). It is shown the light-source, the two lenses (collimator and telescope lens) of MAPS, two Star Enlargers with the pyramids and the pupil-reimager. The plane labeled “focal plane” is the plane labeled “feed to MANU-CHAO” in figure 2.

F/32 to around F/200. However, this cannot be done for the complete field, because the focal plane and thus all the optics behind the pyramids would also have to be increased by a factor of ≈ 6 . For this reason, the F-ratio is increased for each pyramid individually with a so-called Star Enlarger. Each such Star Enlarger consists of two lenses and the pyramid mounted on one single support structure (see fig. 4). The single Star Enlargers can each be moved with four manual linear stages to the position of the Guide-Stars in the field in order to focus the light of the single Guide-Stars on the tip of the respective pyramids.

For a layer-oriented GLAO system, the wavefront sensor camera is focused on the pupil of the system,

therefore the pupil images of the four pyramids overlap on the detector (see fig. 4). To achieve optimal overlap, the tilt of each single Star Enlarger can be adjusted with the manual linear stages. For MANU-CHAO the pupil-reimager can be focused, to conjugate the detector also to different altitudes above the pupil plane.

Considering the size of the CCD pixels and the beam diameter, the pupil images are sampled with 64×64 pixels. However, to match the number of subapertures to the number of actuators and to keep the aliasing noise caused by small mis-alignments small, we usually used a binning of 4×4 and thus 16×16 subapertures.

2.6. Control Software

For controlling the overall system and the individual hardware components, a dedicated software package CARMA (“Control And Reconstruction software for Multi-conjugate Adaptive Optics”) was developed. It is completely GUI-based to adjust the settings and control the CCD-cameras, Deformable Mirror and MAPS for each component individually. It also contains algorithms for the control of the AO loop, like extracting the pupils from the wavefront sensor camera images, calculating the wavefront slopes, calibration & reconstructing of the modal decomposition and calculating the required DM driving voltages. Furthermore it contains some debugging and analysis tools and allows the real-time display of various data like WFS & science camera images, wavefront slopes, residual & applied modal coefficients, residual & applied wavefront, DM voltages and modal covariances.

In order to make it easily editable and to make it possible to quickly and easily implementation new control concepts (like e.g. Kalman filtering), we decided to implement this software package in IDL. For our lab setup, the speed limitation by doing so is not a problem, because the loop frequency is limited by the used CCD cameras to around 5 Hz. All the required calculations can be done during the exposure time of the cameras and thus do not further reduce the loop frequency. Furthermore we have the possibility to continuously adjust the rotation speed of the phasescreens and thus setting the desired wind-speeds relative to the loop frequency.

3. MEASUREMENTS

3.1. Principle

One important verification step of a new AO system is to compare the obtained measurements with a reference. In our case, we compared the reconstructed wavefront aberrations with the measurements made with a commercial interferometer (FISBA). In figure 5 a comparison between these two measurement methods can be seen. The good matching between the measurements of the reference (FISBA) and the reconstructed wavefront from the measurements of MANU-CHAO is obvious, yielding a correlation of around 85%. This gives us confidence that the measurements obtained below are correct and reliable.

But even more than the correlation to a reference in open-loop, the quality of the correction in closed-loop operation is a measure for the performance of an AO system. In figure 6, a comparison of the PSF of the science channel in open-loop (no correction) and closed-loop (with correction) is shown. Without correction, the image is seeing-limited, with a FWHM of the PSF of around $0.5''$. When correcting 36 Zernike modes, the FWHM of the PSF is reduced to around $0.07''$ and thus almost diffraction-limited for this system. The fact that we're using a light-source with a wavelength of 835nm for the science channel, results in a rather modest achievable Strehl-ratio of around 14% in closed-loop operation.

3.2. Calibration Issues

As usual for an Adaptive Optics system operated in modal control, the control loop was calibrated by applying successively the single modes to the DM and measure the response of the wavefront sensor for each of these modes:

$$\mathbf{g} = \mathbf{I} \cdot \mathbf{m} \quad \implies \quad \mathbf{m} = \mathbf{R} \cdot \mathbf{g}. \quad (1)$$

Here \mathbf{g} is a vector containing the measured wavefront gradients and \mathbf{m} is a vector with the single modal coefficients. During calibration, the interaction matrix \mathbf{I} is measured and used to compute the reconstruction matrix \mathbf{R} , which is then employed in closed-loop operation to reconstruct from the measured wavefront gradients the modal decomposition of the wavefront. Due to the limited number of subapertures of the WFS and actuators

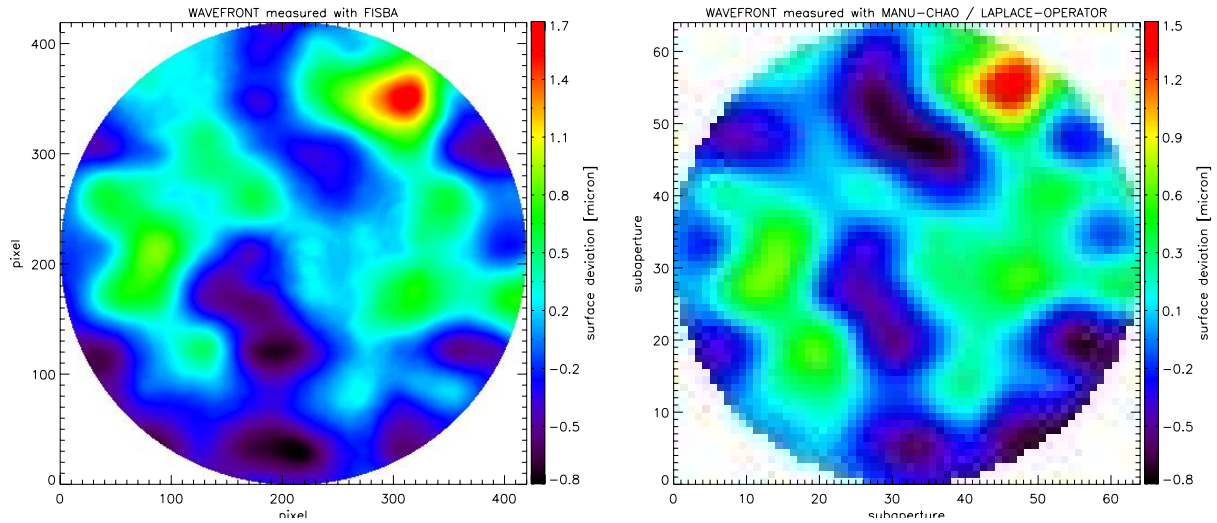


Figure 5. The wavefront as measured with the FISBA interferometer (left) and with MANU-CHAO (right), showing the very good matching of the two measurement methods, with a correlation of $\approx 85\%$.

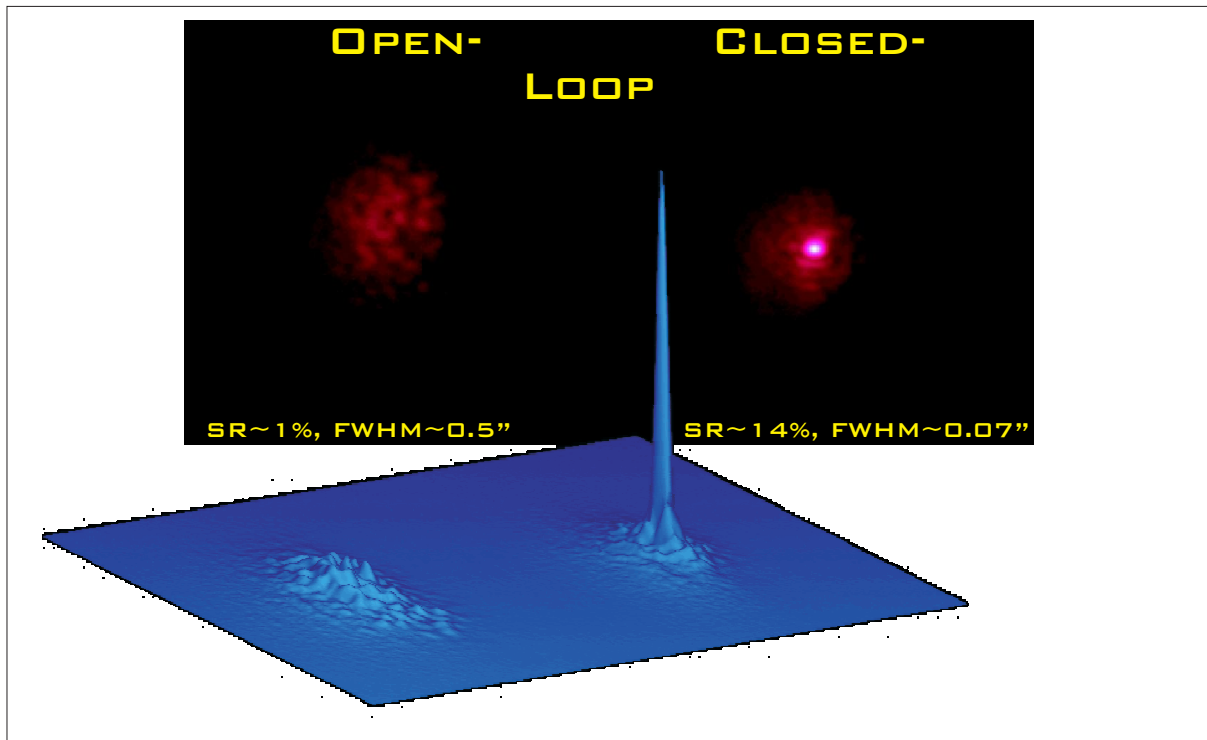


Figure 6. The observed PSF of the science object in open-loop (left panel) and closed-loop (right panel) when using all four pyramids in optical co-addition mode and one phasescreen conjugated to the pupil. Using one phasescreen, the seeing is $\approx 0.5''$, but when correcting 36 Zernike modes, the FWHM of the PSF is decreased to almost diffraction-limited $0.07''$. Since we use a light-source for the science channel with a rather short wavelength of 835nm, we can achieve only a modest Strehl-ratio of around 14% in closed-loop. The PSF images in the top panel are sqrt-contrast stretched to highlight the surrounding halo.

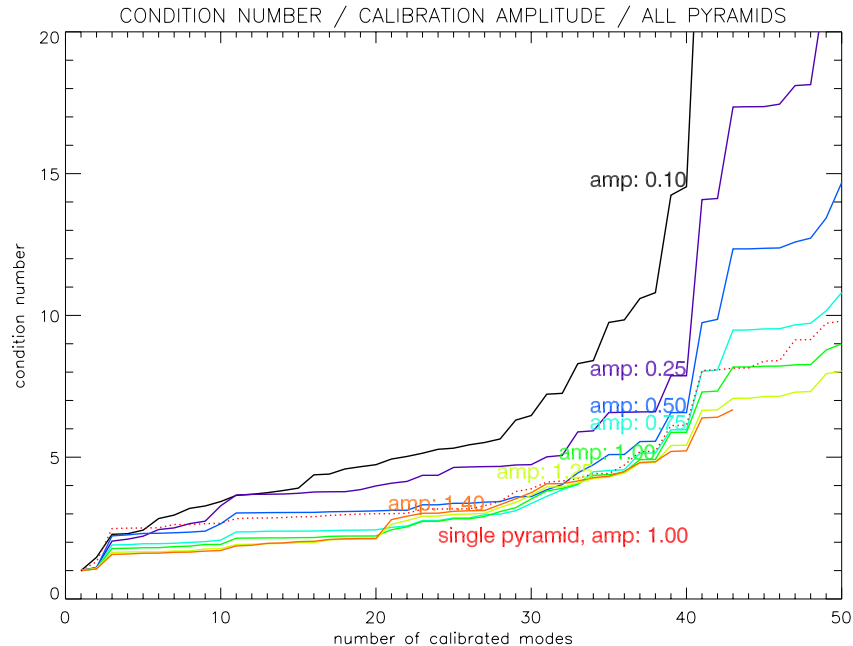


Figure 7. The condition number when using all 4 pyramids, versus the number of calibrated modes. The condition number depends slightly on the used amplitude for the calibration, and steeply increases when using more than 40 modes. Using a calibration amplitude of 0.75 or more (in arbitrary units), the modes are well represented by the DM, the condition number thus remains similar for higher calibration amplitude.

on the DM, only a limited number of modes can be reconstructed. A measure for the maximum useful number of modes is the condition number of the measured interaction matrix. It is defined as the ratio of the largest to the smallest singular value of a matrix. If two modes result in similar gradients (either because due to the limited number of actuators, their representation by the DM is very similar, or because due to the limited number of subapertures, the wavefront-sensor cannot discern them), then the condition number gets rather large and the retrieved reconstruction matrix \mathbf{R} gets close to being singular. In such a case, numerical round-off errors dominate the reconstruction process, resulting in a dramatic decrease of the performance.

As can be seen in figure 7, the condition number depends on the amplitude of the calibration modes and steeply increases when using more than 40 modes. Using these results, we usually calibrated with 39 modes and an amplitude of 1.0 (in arbitrary units). We also verified that the condition number when using all 4 pyramids in optical co-addition mode, is comparable to when using just one pyramid.

3.3. Layer-transfer functions

An important point for MCAO systems is the influence of the non-conjugated turbulent layers on the measurement and correction of the conjugated layers. This has influences on the overall performance of the system and especially on the uniformity of the Strehl-ratio over the field-of-view. To characterize this effect, so-called layer-transfer functions $T(f, \Delta h)$ are defined, which describe how well wavefront aberrations with a spatial frequency f created in a layer at an altitude Δh from the conjugation plane are seen. In the case that the positions of the guide-stars are known and they all have the same brightness, the $T(f, \Delta h)$ can be calculated analytically.²³

To measure this effect in closed-loop, we placed one single phasescreen at different altitudes and left the WFS and DM conjugated to the pupil. When running the system in closed loop, the filtering effect on the resulting Strehl-ratio and FWHM of the PSF can be determined (see fig. 8). Since due to the lack of availability of suitable lab cameras for the near-infrared, we use a wavelength for the science channel of 835nm, the achievable Strehl-ratio is rather low. For a Strehl-ratio of below 10 – 15% there is no longer an easy relationship between

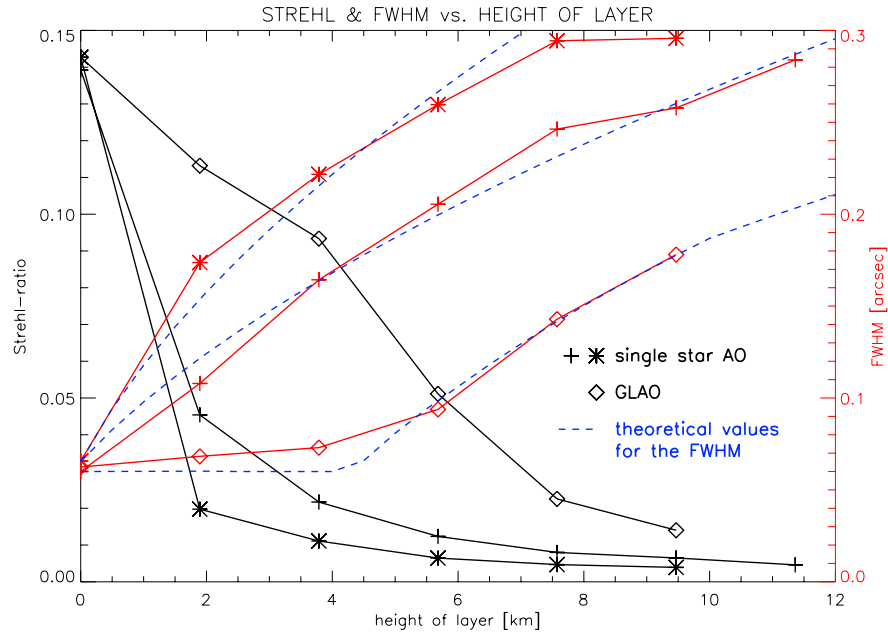


Figure 8. The measured Strehl-ratio and FWHM of the PSF as a function of the height of the phasescreen above the conjugation plane of the WFS / DM combination. For the GLAO case, the science object was placed in the middle of the guide-star asterism ($35'' \times 40''$). For the classical AO, the science object was $17''$ and $20''$ away from the guide-star, respectively.

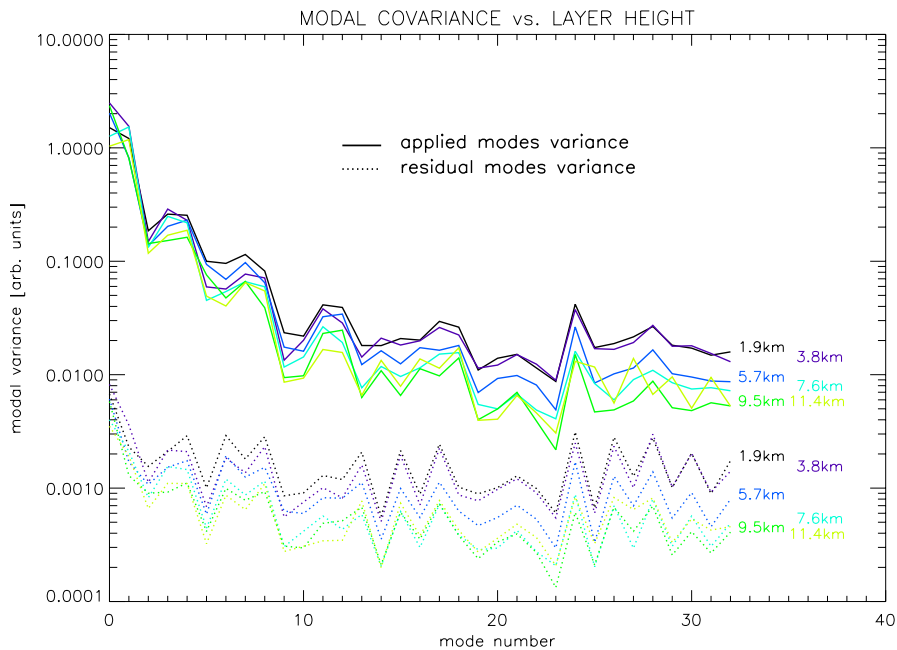


Figure 9. The measured residual and applied modal variance for various heights of the phasescreen above the conjugation plane of the WFS / DM combination in closed-loop. We used only four stars in a rather narrow field-of-view ($35'' \times 40''$), thus the filtering effect is rather small.

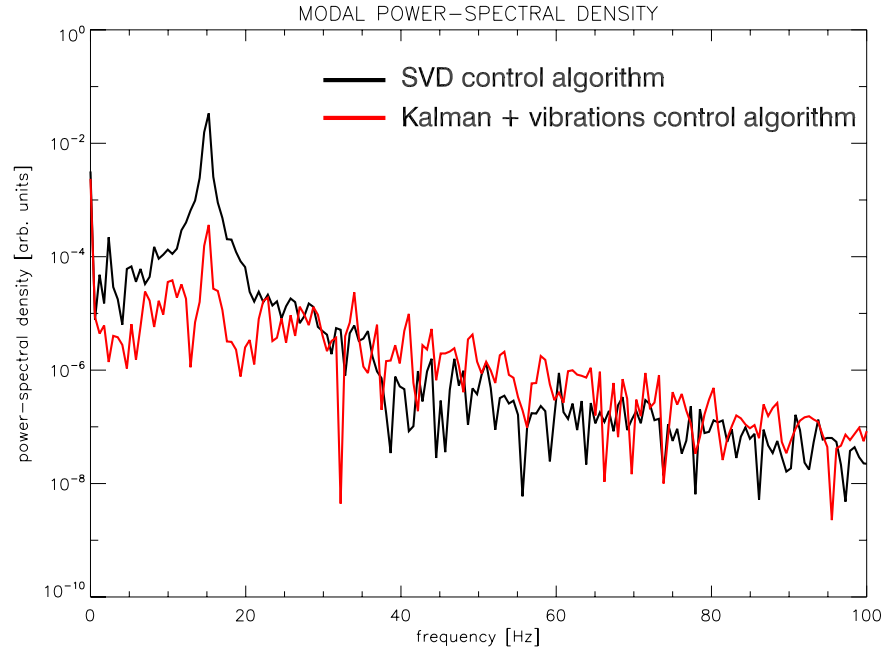


Figure 10. The power spectral density of the residual tilt mode in the presencene of vibrations with a frequency of 15Hz for a loop frequency of 300Hz. Compared to the standard SVD algorithm, the power in these vibrations is damped by a factor of ≈ 100 when using the Kalman filter.

the RMS of the wavefront aberrations and the Strehl-ratio. In such a case, the FWHM W of the PSF is a better measure for the performance of the system:

$$W = 0.98 \frac{\lambda}{r_0} \quad \text{and} \quad \sigma^2 = 1.03 \cdot \left(\frac{D}{r_0} \right)^{5/3} \quad (2)$$

with the Fried Parameter r_0 , which can be determined from the diameter D of the pupil and the variance of the wavefront aberrations σ^2 .

This filtering effect can also be examined for the single Zernike modes by determining the time-averaged variance of the modal coefficients as a function of the altitude difference Δh between the turbulent layer and conjugation plane of the WFS / DM combination. As can be seen in figure 9, the filtering effect is stronger for the higher order Zernike modes, because they contain higher spatial frequencies which are filtered more efficiently.

3.4. Kalman Filter

As described above, MANU-CHAO contains all the components of a real AO system, including dynamic turbulence and telescope simulator, making it an ideal testbed to test new control algorithms / concepts for AO. It can be used to examine the performance increase of recently developed wavefront reconstruction and control algorithms in a real system and determine the effects of mechanical inaccuracies, small optical mis-alignments and the sensitivity on the accuracy of the additionally required quantities.

Considering the fact that vibrations significantly reduce the performance of most AO system (like NACO²⁴ or AO@MMT²⁵), we decided to test the capabilities of the Kalman filter to filter out such vibrations. The details of the theory of Kalman filtering is not presented here, a nice introduction to its application to Adaptive Optics can be found in Le Roux et al.,²⁶ an extension to include also vibrations and static aberrations in Petit et al.²⁴ For MANU-CHAO we used the same algorithm, with slight modifications to account for the small differences in the calibration procedure. Le Roux et al.²⁶ formulated the Kalman filter for a calibration based on the influence functions of the single actuators, we used a calibration based on Zernike modes.

To add vibrations on single Zernike modes in MANU-CHAO, a separate loop is running, which applies additionally – independently of the AO control loop – a sinusoidal amplitude variation of single modes to the DM. For the AO control loop we then either used the SVD reconstruction matrix multiplication (as in eqn. 1) or the Kalman filter, with the known frequency of the vibrations as an input. The required average modal covariance matrix and process noise matrix were measured in open-loop without vibrations, the measurement noise matrix was determined from the auto-correlation $AC(\Delta T)$ of the measured wavefront slopes.²⁷

In figure 10, the power-spectrum of the tilt mode with the additional vibrations (with an amplitude PV of 0.15 micron and a frequency of 15Hz for a loop-frequency of 300Hz) is plotted. As can be seen, at the frequency of the vibrations, there is a distinct peak, which is left almost un-filtered by the SVD reconstruction algorithm. On the contrary, when using the Kalman-filter, the residual energy in these vibrations is reduced by a factor of ≈ 100 . This results in a Strehl-ratio of 13.6% for the Kalman filter and 11.6% for the SVD algorithm, as compared to 14.0% in the case without additional vibrations.

4. CONCLUSION

We presented a laboratory setup of a Ground-Layer Adaptive Optics (GLAO) system containing all the required components like light-source, dynamic turbulence simulator, Deformable Mirror, wavefront sensor unit, science channel and sophisticated control software for extensive closed-loop tests. The single components were described in detail and the principle of the layer-oriented approach by using four pyramids in optical co-addition mode is shown.

Open-loop measurements done with this system show a high correlation factor ($\approx 85\%$) of the determined wavefront aberrations with the ones as measured by a commercial interferometer, confirming the good alignment and correct control of the system. Some first results obtained with this system in closed-loop operation show the increase in performance, in terms of Strehl-ratio and FWHM, of such a GLAO system as compared to a single-star off-axis AO system. In the case of a GLAO system, the FWHM of the PSF is reduced by a factor 1.5 to 2.0 and matches very well the theoretical predictions determined from layer transfer functions. Furthermore, the filtering effect of non-conjugated layers was examined for the single Zernike modes separately by analysing the temporal variance of the modal coefficients.

We also described first results obtained with a Kalman filter for the control of the AO loop in the presence of additional vibrations. The temporal power-spectrum of the applied modes shows that the power in the added vibrations is filtered by a factor of around 100 as compared to the standard SVD algorithm, resulting in a significant increase of the achievable Strehl-ratio.

The MANU-CHAO system with all the required components for closed-loop operation, together with the modal control software CARMA make it thus an ideal testbed to compare new control algorithms, experiment with the star- & layer-oriented approach for GLAO systems, etc. under easy manageable lab conditions with adjustable and repeatable atmospheric conditions.

ACKNOWLEDGEMENTS

The work was funded by the Alexander von Humboldt Foundation through the Wolfgang Paul Prize.

We are grateful to Florian Briegel, Frank Kittmann & Udo Neumann for their help in developing the CARMA software package, Peter Bizenberger for many advices on optical design, Felix Hormuth & Stefan Hippler for their support on MAPS, and Lars Mohr & Karl Wagner for taking care of the electronics. Furthermore we want to thank the whole team of the mechanical workshop at the MPIA, especially Ralf-Rainer Rohloff, Norbert Muench, Armin Boehm and Wolfgang Sauer, for the design and manufacturing of all the required hardware components.

REFERENCES

1. H. W. Babcock, "The Possibility of Compensating Astronomical Seeing," *PASP* **65**, p. 229, 1953.
2. J. Beckers, "Increasing the Size of the Isoplanatic Patch with Multiconjugate Adaptive Optics," in *Very Large Telescopes and their Instrumentation, ESO Conference and Workshop Proceedings*, 1988.

3. F. Rigaut, B. Ellerbroek, and R. Flicker, "Principles, limitations, and performance of multiconjugate adaptive optics," in *SPIE*, 4007, p. 1022, 2000.
4. R. Avila, E. Masciadri, J. Vernin, and J. Sánchez, "Generalized SCIDAR Measurements at San Pedro Mártir. I. Turbulence Profile Statistics," *PASP* **116**, p. 682, 2004.
5. S. Egner, E. Masciadri, D. McKenna, T. M. Herbst, W. Gaessler, and etc., "G-SCIDAR measurements on Mt. Graham – recent results," in *SPIE*, 6272, 2006.
6. J.-L. Prieur, G. Daigne, and R. Avila, "SCIDAR measurements at Pic du Midi," *A&A* **371**, p. 366, 2001.
7. A. Tokovinin, J. Vernin, A. Ziad, and M. Chun, "Optical Turbulence Profiles at Mauna Kea measured by MASS and SCIDAR," *PASP* **117**, p. 395, 2005.
8. F. Rigaut, "Ground Conjugate Wide Field Adaptive Optics for the ELTs," in *BCAO*, p. 11, 2002.
9. A. Athey, S. Shtetman, P. Schechter, and B. Lane, "The GMT ground-layer AO experiment at the Magellan telescopes," in *SPIE*, 5490, p. 960, 2004.
10. N. Hubin, M. L. Louarn, R. Conzelmann, B. Delabre, E. Fedrigo, and R. Stuik, "Ground layer AO correction for the VLT MUSE project," in *SPIE*, 5490, p. 846, 2004.
11. T. Morris, P. Berry, T. Butterley, P. Clark, C. Dunlop, R. Myers, C. Saunter, and R. Wilson, "A ground-layer AO system demonstrator for the William Herschel Telescope," in *SPIE*, 5490, p. 891, 2004.
12. A. Tokovinin, S. Thomas, B. Gregory, N. van der Blik, P. Schurter, R. Cantarutti, and E. Mondaca, "Design of ground-layer turbulence compensation with a Rayleigh beacon," in *SPIE*, 5490, p. 870, 2004.
13. R. Ragazzoni, J. Farinato, and E. Marchetti, "Adaptive optics for 100-m-class telescopes: new challenges require new solutions," in *SPIE*, 4007, p. 1076, 2000.
14. J. Farinato, R. Ragazzoni, and E. Diolaiti, "Novel techniques concerning MCAO: trying to overcome fundamental limitations," in *SPIE*, 5490, p. 1229, 2004.
15. A. Tokovinin, "Seeing Improvement with Ground-Layer Adaptive Optics," *PASP* **116**, p. 941, 2004.
16. M. Nicolle, T. Fusco, V. Michau, G. Rousset, A. Blanc, and J.-L. Beuzit, "Ground layer adaptive optics: analysis of the wavefront sensing issue," in *SPIE*, 5490, p. 858, 2004.
17. C. Baranec, M. Lloyd-Hart, J. Codona, and N. Milton, "Sky demonstration of potential for ground-layer adaptive optics correction," in *SPIE*, 5169, p. 341, 2003.
18. S. Hippler, W. Brandner, D. Butler, S. Egner, T. Henning, and F. Hormuth, "The MPIA multipurpose laboratory atmospheric turbulence simulator," in *SPIE*, 6272, 2006.
19. W. Gaessler, C. Arcidiacono, S. Egner, T. Herbst, D. Andersen, H. Baumeister, P. Bizenberger, H. Boehnhardt, F. Briegel, M. Kuerster, W. Laun, L. Mohr, B. Grimm, H.-W. Rix, R.-R. Rohloff, R. Soci, C. Storz, W. Xu, R. Ragazzoni, P. Salinari, E. Diolaiti, J. Farinato, M. Carbillet, L. Schreiber, A. Eckart, T. Bertram, C. Straubmeier, Y. Wang, L. Zealouk, G. Weigelt, U. Beckmann, J. Behrend, T. Driebe, M. Heininger, K.-H. Hofmann, E. Nussbaum, D. Schertel, and E. Masciadri, "LINC-NIRVANA: MCAO toward Extremely Large Telescopes," *Comptes Rendus Physique* **6**, p. 1129, 2005.
20. S. Egner, W. Gaessler, T. Herbst, R. Ragazzoni, R. Stuik, D. Andersen, C. Arcidiacono, H. Baumeister, U. Beckmann, J. Behrend, T. Bertram, P. Bizenberger, H. Boehnhardt, E. Diolaiti, T. Driebe, A. Eckhardt, J. Farinato, M. Kuerster, W. Laun, S. Lorigi, V. Naranjo, E. Nussbaum, H.-W. Rix, R.-R. Rohloff, P. Salinari, R. Soci, C. Straubmeier, E. Vernet-Viard, G. Weigelt, R. Weiss, and W. Xu, "LINC-NIRVANA: the single arm MCAO experiment," in *SPIE*, 5490, p. 924, 2004.
21. R. Stuik, S. Hippler, M. Feldt, J. Aceituno, and S. Egner, "Characterization of deformable mirrors for high-order adaptive optics systems," in *SPIE*, 5490, p. 1572, 2004.
22. S. Egner, "Xinetics DM test report," Tech. Rep. LN-MPIA-FDR-TN-AIT-001, MPIA, 2005.
23. M. Owner-Petersen and A. Gontcharov, "Multi-conjugate Adaptive Optics for Large Telescopes Analytical Control of the Mirror Shapes," *JOSA* **19**, p. 537, 2002.
24. C. Petit, F. Quiros-Pacheco, J.-M. Conan, C. Kulcsár, H.-F. Reynaud, T. Fusco, and G. Rousset, "Kalman filter based control for Adaptive Optics," 5490, p. 1414, SPIE, 2004.
25. M. Kenworthy (private communications).
26. B. L. Roux, J.-M. Conan, C. Kulcsar, H.-F. Raynaud, L. Mugnier, and T. Fusco, "Optimal control law for classical and multiconjugate adaptive optics," *JOSA* **21**, p. 1261, 2004.
27. R. Weiß, *Point Spread Function Reconstruction for the Adaptive Optics System ALFA and its Application to Photometry*. PhD thesis, University of Heidelberg, 2003.